Sintering and properties of Ultra High Temperature Ceramics for aerospace applications

J.F. Justin

Sintering and properties of Ultra High Temperature Ceramics for aerospace applications

J.F. Justin
Onera Châtillon
Composite Materials and Structures Department
E-mail: jean-francois.justin@onera.fr

ABSTRACT

The Ultra High Temperature Ceramics (UHTCs) represent a very interesting family of materials and therefore they are the subject of increasing attention from different engineering sectors and notably the aerospace industry. Indeed, hypersonic flights, re-entry vehicles, propulsion applications and so on, require new materials that can perform in oxidizing or corrosive atmospheres at temperatures higher than 2000°C and sometimes, for long life-time. To fulfil these requirements, UHTCs seems to be one of the most promising candidates and among this family, ZrB_2 and HfB_2 based composites are the most attractive. Thus, in diborides-based compounds, at temperatures above 1600°C, the oxidation resistance is generally much better than that of traditional SiC-based ceramics thanks to the formation of multi-oxide scales composed of a refractory oxide (skeleton) and a glass component.
Since 2006, Onera actively takes part in several programmes to investigate such materials as well for hypersonic civil flights as for propulsion systems. Diverse manufacturing processes and compositions have been studied in theses projects.
In this paper, we present different type of materials developed for some specific applications: leading edges, air intakes, uncooled injectors of future hypersonic civil aircrafts flying up to Mach 6.

1 INTRODUCTION

It is well known that silicon-based ceramics and protected C/C composites exhibit good oxidation resistance, but only up to ~1600°C, and their thermal cycling lifetimes are modest. So, the development of structural materials for use in oxidizing and rapid heating environments at temperatures above 1600°C is therefore of great importance for engineering. Studies have revealed that Ultra High Temperature Ceramics were particularly interesting to fulfil these requirements [1]. UHTCs are compounds made of borides, carbides and nitrides such as ZrB_2, HfB_2, ZrC, HfC, TaC, HfN which are characterized by high melting points (table 1), high hardness, chemical inertness and relatively good resistance to oxidation in severe environments [2][3]. Diborides of the group IVb are the most resistant to oxidation and among these compounds; HfB_2 is the best, followed by ZrB_2. However, the use of single-phase materials is not sufficient for high-temperature structural applications. Thus, many additives such as Nb, V, C, disilicides and SiC were evaluated to improve the resistance to oxidation. Of these additives, SiC seemed to be particularly valuable and values around 20 vol% were judged optimal for hypersonic vehicles applications. Currently, many groups in the U.S., Japan, China, India and in Europe are studying UHTC systems to improve their resistance to oxidation [4][5][6][7].

Material	Crystal structure	Density (g/cm^3)	Melting temperature (°C)
HfB_2	Hexagonal	11.2	3380
HfC	Face-centered cubic	12.76	3900
HfN	Face-centered cubic	13.9	3385
ZrB_2	Hexagonal	6.1	3245
ZrC	Face-centered cubic	6.56	3400
ZrN	Face-centered cubic	7.29	2950
TiB_2	Hexagonal	4.52	3225
TiC	Cubic	4.94	3100
TiN	Face-centered cubic	5.39	2950
TaB_2	Hexagonal	12.54	3040
TaC	Cubic	14.50	3800
TaN	Cubic	14.30	2700
SiC	Polymorph	3.21	Dissociates 2545

Table 1: Properties of some UHTCs

Moreover, diborides have also higher thermal conductivity than carbides and nitrides, which gives them good thermal shock resistance and makes them ideal for many high-temperature thermal applications. For a leading edge

for example, a high thermal conductivity reduces thermal stress within the material by lowering the magnitude of the thermal gradient inside the part. Furthermore, it allows energy to be conducted away from the tip of the piece and re-radiated out of the surfaces of the component with lower heat fluxes [8]. Diboride-based UHTCs exhibit also high electrical conductivity, which permits for example to manufacture complex shape components by Electrical Discharge Machining [9].

Over the past seven years, Onera has carried out several activities on UHTC materials. Among them, this paper is an outline of the work which has been done within the framework of the European Projects ATLLAS (Aerodynamic and Thermal Load Interactions with Lightweight Advanced Materials for High Speed Flight) and ATLLAS II (Aero-Thermodynamic Loads on Lightweight Advanced Structures II). These projects [10][11], led by ESA-ESTEC, consist of a consortium of several European partners from industry, research institutions and universities. Within these programmes, ONERA has the objective of investigating and manufacturing UHTC materials to allow for the designing of sharp leading edges or air intakes [12][13] but also in the second project for an uncooled injector. Indeed, for hypersonic vehicles, performance improvement (lift-to-drag ratio in particular) requires slender aerodynamic shapes with sharp leading edges. However, the thinner the leading edge radius, the higher the temperature! In addition, fuel injectors used within airbreathing propulsion units of any hypersonic vehicle have to face a severe thermo-mechanical environment and they need currently to be cooled to survive. So, the development of sharp uncooled UHTC injectors would be a real benefit for efficiency.

In the first ATLLAS programme, the study was focused on compositions that could be sintered by hot pressing [14][15] (with expected densification temperatures between 1600 and 1800°C). On the other hand, in ATLLAS II, the need to obtain higher temperature capabilities, made us choose a new manufacturing method called Spark Plasma Sintering (SPS) or Field Assisted Sintering Technology (FAST) which allows the selection of others compositions. It is important to notice that very rapid heating times and short sintering cycles can be achieved using this modified hot pressing process in which electric current runs through the pressing mould and the component [16]. In addition, its operation is easy and it enables ceramics to become fully dense at comparatively low temperatures and with limited grain growth.

2 EXPERIMENTAL PROCEDURE

2.1 Material and processing

The following compositions have been investigated in ATLLAS or they are currently under investigation in ATLLAS II (the first three in ATLLAS and the last four in ATLLAS II):

- ZrB_2 (60 vol%) + SiC (20 vol%) + $TaSi_2$ (20 vol%)
- HfB_2 (60 vol%) + SiC (20 vol%) + $TaSi_2$ (20 vol%)
- ZrB_2 (80 vol%) + SiC (20 vol%)
- HfB_2 (80 vol%) + SiC (20 vol%)
- HfB_2 (77 vol%) + SiC (20 vol%) + Y_2O_3 (3 vol%)
- ZrB_2 (92.5 vol%) + SiC (7.5 vol%)

To obtain theses compositions, commercially available ZrB_2, HfB_2, SiC, $TaSi_2$ and Y_2O_3 powders (table 2) were used as raw materials. To reduce particle size and promote intimate mixing, starting powders were milled in cyclohexane in a high-density polyethylene tank using different milling media (Si_3N_4, ZrO_2 or WC). Solvent was dried using rotary evaporation to minimize segregation and finally, the mixtures were sieved to avoid agglomeration.

Starting powder	Particle size (µm)	Grade / supplier	Purity (%)
ZrB_2	8.17	Z-1031 / Cerac	99.5
	2.83	Grade B / H.C. Starck	> 97.8
HfB_2	1.99	H-1002 / Cerac	99.5
	7.57	Grade A / H.C. Starck	> 96.9
SiC	0.60	BF12 / H.C. Starck	> 98.5
$TaSi_2$	6.54	T-1016 / Cerac	99.5
Y_2O_3	< 5.0	Ampère Industrie	> 99.99

Table 2: Size, grade and purity of starting powders

In the selected compositions, silicon carbide is used firstly to enhance resistance to oxidation, secondly to promote densification by restricting the grain growth of diborides, and lastly to lower their sintering temperature [17]. For tantalum disilicide additions, the objectives are to increase oxidation resistance and to reduce the sintering temperature of the powder blends [17][18] (indeed, the melting temperature of the $TaSi_2$ is "only" 2400°C). The addition of Ta to the system reduces the concentration of oxygen vacancies and decreases oxygen transport through the growing oxide scale and thus lowers the oxidation rate. Furthermore, Ta additions increase the oxide scale

adhesion by phase stabilization. Concerning yttrium oxide, it is a sintering aid which can lead to high temperature solid solutions with hafnia and zirconia and improve the oxidation resistance.
Milled powders were densified by two methods: Hot Pressing (in ATLLAS) and Field Assisted Sintering Technology (manufacturing phase always in progress in ATLLAS II). According to compositions, we have applied different densification parameters to obtain UHTC monolithic plates and discs (Figure 1). A synthesis of these parameters is presented in Table 3.

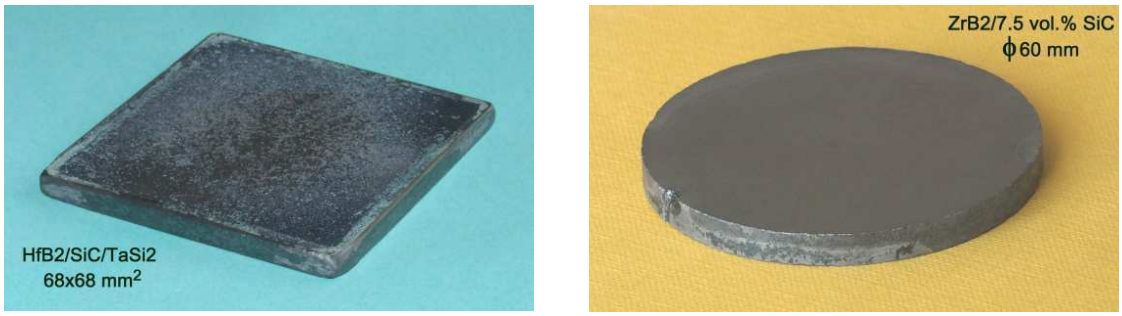

Figure 1 : Aspect of monolithic UHTC materials.

Parameter	HP	FAST
Sintering temperature	1700 < T < 1800°C	1900 < T < 2200°C
Dwell Time	2 hours	3 to 15 min
Uniaxial Pressure	27 MPa	28 to 30 MPa
Atmosphere	Argon	Vacuum
Graphite dies	36x36, 45x45 and 68x68 mm^2	∅ 20, 30, 60 mm

Table 3 : Sintering conditions for each manufacturing process

2.2 Characterizations

The bulk density was determined by the Archimedes method. Phase composition was determined by X-ray diffractometry. The microstructure of each monolith was characterized using scanning electron microscopy (SEM) along with energy dispersive spectroscopy (EDS) for chemical analysis. Samples were cut into bars measuring ~35.40 x 5.20 x 1.75 mm^3 for flexural strength determination (at different temperature) and Young's modulus characterization (at room temperature). Each bar was ground and polished with diamond slurries down to 1/4µm finish. The edges of all the specimens were chamfered to minimize the effect of stress concentration. The flexural stress (σ_f), the modulus of elasticity in bending (E_f) and the flexural strain (ε_f) were measured by a three-point bending method with a cross-head speed of 0.3 mm/min and a span of 30 mm. Young's moduli were deducted by impulse excitation of vibration using a Grindosonic MK5 apparatus [19]. Fracture toughness (K_{1c}) and hardness (Hv) determinations were evaluated at room temperature by Vickers indentation (load = 98 N, dwell time of 15 s) on polished sections (1/4µm finish). The fracture toughness was estimated by crack length measurement of the radial crack pattern formed around Vickers indents [20]. The thermal expansion behaviour has been characterized between room temperature and 1300 or 1450°C by using an Adamel Lhomargy DI.24 dilatometer (under argon flow). The thermal conductivity (λ) was calculated from the correlation functions of thermal diffusivity (D), specific heat capacity (Cp) and density (ρ) according to the formula:

$$\lambda(T) = D(T) \times \rho(T) \times Cp(T) \qquad \text{Eq. I}$$

The correlations for density were deduced from the CTE measurements. Diffusivity and specific heat were determined by a flash laser technique [21] from room temperature to 1200°C (under argon) on 20 mm in diameter and 2 mm-thick discs. Total hemispherical emissivity (ε) were deducted from spectral thermal emissivity measurements [22] and the assessment of each material was done on parallelepiped samples (16 x 8 x 2 mm^3), from 200 to 800°C, under argon, before and after an oxidation treatment at 1000°C. The thermal shock behaviour and the long time resistance under oxidative atmosphere and high temperature have been assessed by thermal treatments of several samples at 1000°C under stagnant air at atmospheric pressure. The thermal and chemical resistance of some materials has been investigated on disc-shaped samples (Ø 26.5 mm, e = 4 mm) under high-enthalpy hypersonic flow in an arc-jet facility at DLR Cologne (L2K) [23].

3 RESULTS AND DISCUSSION

3.1 Densification level and microstructure

High densifications rates were obtained on sintered monoliths. For all compositions, the open porosities were lower than 1 % and their densification rates were approximately 98 % of the theoretical value. Furthermore, very fine

microstructures, in particular for compositions with $TaSi_2$, were obtained with good homogeneity and a small grain size (Figure 2). We noticed that $TaSi_2$ seemed to act as a grain growth inhibitor.
The XRD analysis of the materials showed the peaks associated with the main crystalline phases (ZrB_2, HfB_2, SiC, $TaSi_2$ and Y_2O_3) but also some traces of secondary phases as ZrO_2, HfO_2, SiO_2, HfC and Ta_5Si_3. These phases are located at grain boundaries and are presumably due to the reaction of impurities and matrix during sintering.

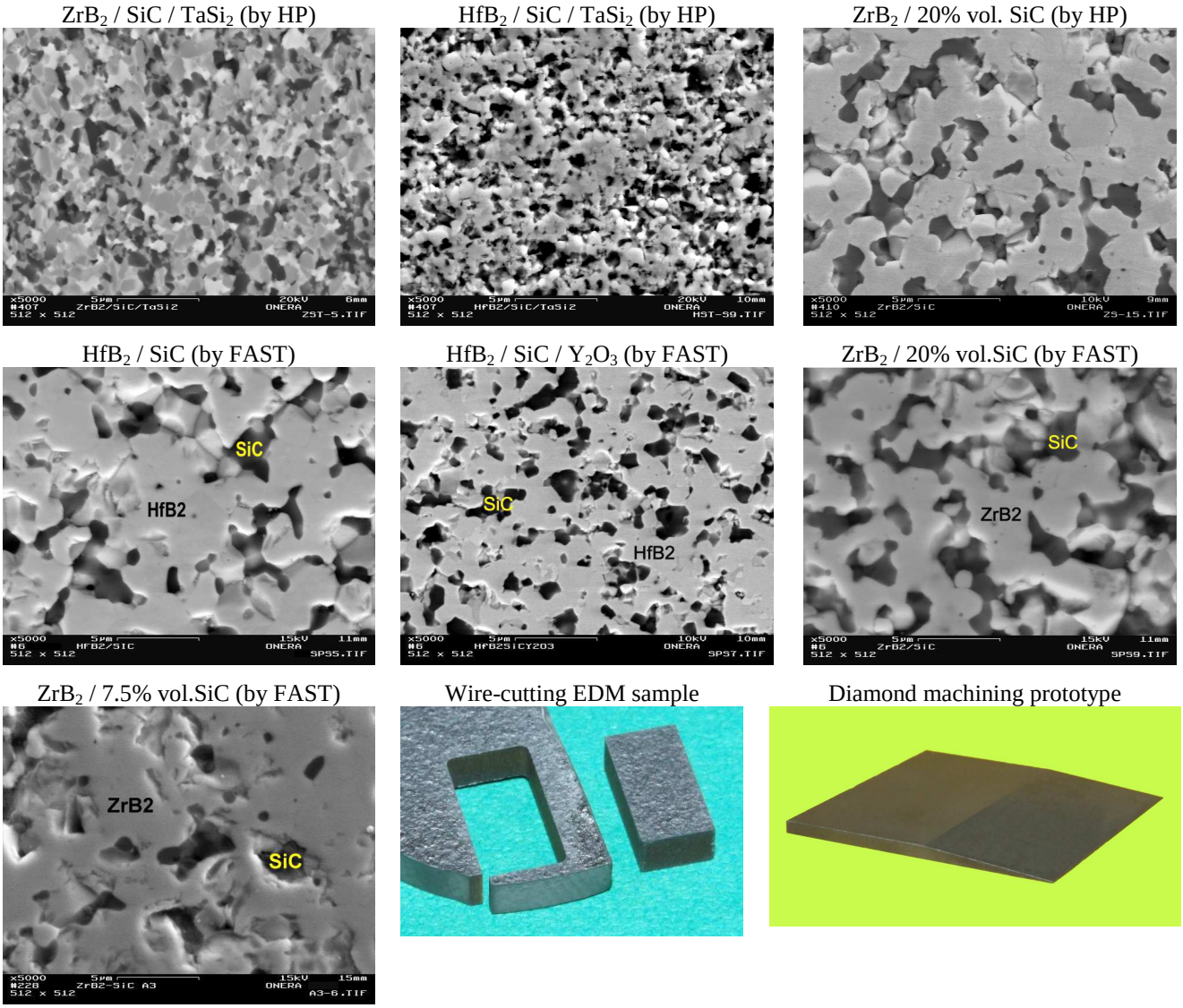

Figure 2 : Microstructure of several compositions and machining trials.

3.2 Machinability

It is well known that materials based on hard and brittle constituents (borides, carbides and silicides) often involve expensive and difficult machining. In our case, thanks to the low electrical resistivity of the compounds, the use of Electrical Discharge Machining was perfectly possible (ρ_{ZrB2} = 6 to 10 µΩ.cm, ρ_{HfB2} = 10 to 16 µΩ.cm, $\rho_{SiC} \sim 10^5$ µΩ.cm and ρ_{TaSi2} = 8 to 46 µΩ.cm [24]). Thus, the selected materials could be easily machined and the surfaces were clean and even (Figure 2). This is one of the important advantages of these materials. It is important to note that, with EDM, complex shapes can also be made using a die-sinking machine, also known as a ram-type, plunge, or vertical erosion machine [25]. Furthermore, we have also demonstrated the good behaviour of the selected materials for machining with the standard techniques (surface grinding with diamond tools for instance). Several samples and prototypes were manufactured with this method. In particular, the feasibility of an air intake prototype with a very thin tip was investigated (Figure 2). As expected, a small radius was obtained (prototype dimensions: length = 40 mm, width = 40 mm, thickness = 1.9 mm and radius ~ 0.15 mm). Thus, it is clearly possible to obtain very sharp pieces and acute angles.

3.3 Mechanical properties

It is important to notice that all the characterizations of the new compositions investigated in ATLLAS II aren't available for the moment but when it was possible the results are presented. Young's modulus, hardness and

toughness of several materials at room temperature are shown in Table 4 and the variation of flexural strength with temperature is indicated in Table 5. The recorded values of the Young's modulus are in good agreement with the expected results [26][27][28]. For information, similar materials have already been presented in the literature and they generally exhibit shear moduli close to 200 GPa and Poisson's ratios around 0.12 - 0.14 [26][29]. Very high levels of hardness and limited levels of toughness have been measured on the investigated compositions. In fact, all the materials exhibit hardness values close to that of tungsten carbide (Hv ~ 19.6 GPa) and toughness similar to that of common silicon nitride (K_{1c} ~ 3.5 - 6 MPa.m$^{1/2}$). SEM observations of the cracks have revealed that both intergranular and transgranular modes of propagation were present. Comparable behaviours are reported in the literature for this type of ceramic [26][27].

Composition	H_{v10} / GPa	K_{1c} / MPa m$^{1/2}$	E / GPa
ZrB_2/SiC/$TaSi_2$ (HP)	18.1 ± 0.4	4.4 ± 0.3	446 ± 9
HfB_2/SiC/$TaSi_2$ (HP)	18.1 ± 0.6	4.6 ± 0.2	498 ± 6
ZrB_2/SiC (HP)	20.9 ± 1.9	4.3 ± 0.2	465 ± 15
HfB_2/SiC (FAST)	17.5 ± 0.3	6.7 ± 0.9	-----
HfB_2/SiC/Y_2O_3 (FAST)	21.9 ± 1.1	3.9 ± 0.3	-----

Table 4 : Hardness, toughness and Young's modulus of several materials

Composition	Property	Test temperature		
		20°C	1000°C	1150°C
ZrB_2/SiC (HP)	σ_f (MPa)	451 ± 90	331 ± 270	286 ± 177
	E_f (GPa)	194 ± 6	137 ± 48	101 ± 48
	ε_f (%)	0.23 ± 0.04	0.23 ± 0.12	0.28 ± 0.04
ZrB_2/SiC/$TaSi_2$ (HP)	σ_f (MPa)	688 ± 79	801 ± 40	864 ± 96
	E_f (GPa)	211 ± 13	181 ± 14	133 ± 13
	ε_f (%)	0.32 ± 0.02	0.45 ± 0.04	0.65 ± 0.02
HfB_2/SiC/$TaSi_2$ (HP)	σ_f (MPa)	869 ± 170	882 ± 146	1055 ± 189
	E_f (GPa)	245 ± 13	203 ± 24	178 ± 22
	ε_f (%)	0.36 ± 0.09	0.43 ± 0.05	0.56 ± 0.13

Tableau 5 : Three point flexural strength (average value ± standard deviation)

Concerning the behaviour in bending, the measured values are very satisfactory except for the ZrB_2/SiC material for which some improvements are necessary. We can observe that for material comprising $TaSi_2$, increasing temperature leads to higher flexural stresses, a strong increase of flexural strains and a moderate decrease in the flexion modulus. It is important to point out that, with these high levels of flexural stress (values over 1200 MPa have even been measured on HfB_2/SiC/$TaSi_2$ samples at 1150°C), it seems possible to develop future UHTC components.

3.4 Thermal and optical properties

3.4.1 Coefficient of thermal expansion (CTE):

The coefficient of thermal expansion (α_{secant} in °C^{-1}) is calculated from the following formula:

$$\alpha = \frac{1}{L_0} \times \frac{\Delta L}{\Delta T} \qquad \text{Eq. II}$$

In our measurements, the reference temperature is room temperature (25°C). The first three compositions investigated below have been characterized from 25 to 1300°C and the last three between 25 and 1440°C. Thus between 25 and 1300 or 1440°C, the average values of CTE are:

- for ZrB_2/SiC (HP) $\alpha_{25-1300°C}$ = 7.2 10^{-06} °C^{-1}
- for ZrB_2/SiC/$TaSi_2$ (HP) $\alpha_{25-1300°C}$ = 7.3 10^{-06} °C^{-1}
- for HfB_2/SiC/$TaSi_2$ (HP) $\alpha_{25-1300°C}$ = 7.4 10^{-06} °C^{-1}
- for ZrB_2/SiC (FAST) $\alpha_{25-1440°C}$ = 7.8 10^{-06} °C^{-1}
- for HfB_2/SiC (FAST) $\alpha_{25-1440°C}$ = 9.3 10^{-06} °C^{-1}
- for HfB_2/SiC/Y_2O_3 (FAST) $\alpha_{25-1440°C}$ = 11.4 10^{-06} °C^{-1}

We have noticed that typical standard deviations on these characterizations are between 0.2 and 0.8 10^{-06} °C^{-1}.

The CTE values are in good agreement with the data available in the literature on similar materials [28][30]. In comparison to advanced CMC (SiC/SiC or C/SiC), these coefficients are quite high and closer to some ceramics like alumina ($\alpha_{0-1000°C}$= 8 10^{-6}°C^{-1}). However, they are twice as low as for metallic materials such as nickel alloys (for Inconel 617 for instance $\alpha_{25-1000°C}$= 16.3 10^{-6}°C^{-1}).

3.4.2 Thermal conductivity (λ):

The thermal conductivity of materials was determined only on monoliths with $TaSi_2$. The values calculated from the correlation functions of thermal diffusivity, specific heat capacity and density are presented in Figure 3. The correlations for λ are given by the following expressions (in these formulas, T is in °C units):

- for $ZrB_2/SiC/TaSi_2$ (HP) $\lambda(T) = 2.6693\cdot10^{-8}\cdot T^3 - 6.0102\cdot10^{-5}\cdot T^2 + 3.0995\cdot10^{-2}\cdot T + 3.6168\cdot10^{+1}$ Eq. III
- for $HfB_2/SiC/TaSi_2$ (HP) $\lambda(T) = 1.7971\cdot10^{-8}\cdot T^3 - 3.8412\cdot10^{-5}\cdot T^2 + 1.6151\cdot10^{-2}\cdot T + 3.2240\cdot10^{+1}$ Eq. IV

From 20 to 1200°C, the thermal conductivities of the characterized materials are higher than 25 $W.m^{-1}.K^{-1}$. In fact, the thermal conductivities of diboride-based UHTC are typically high [31][32], in comparison with those of many other ceramics [33] and are a result of both a lattice (vibrations) and an electronic contribution to phonon transport [34]. These values are also higher than for some alloys and CMC (for example: at 300K, λ= 13.6 $W.m^{-1}.K^{-1}$ for Inconel 617 and λ~ 14.5 $W.m^{-1}.K^{-1}$ for a standard C/C-SiC). This ability to easily transport heat is one of the most important advantages of these materials. Indeed, their high conductivity allows heat to be conducted from a high heating area to a region of lower heating, where it is then re-radiated into the atmosphere. Furthermore, their high level of conduction gives them good thermal shock resistance.

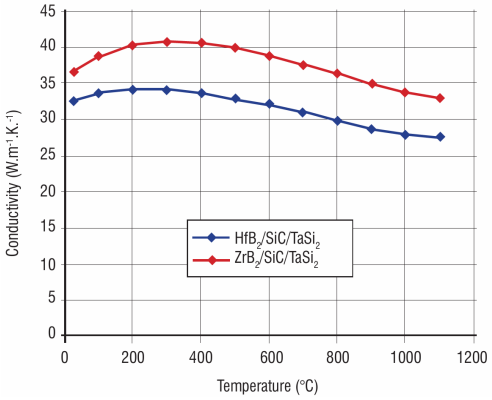

Figure 3 : Thermal conductivity.

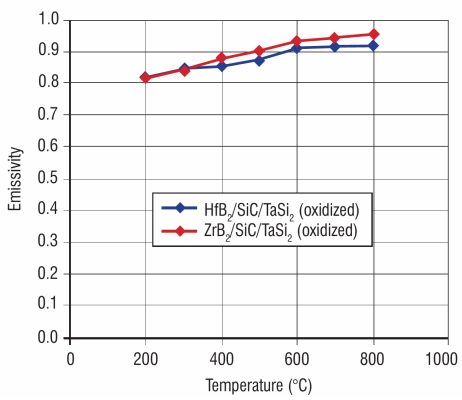

Figure 4 : Emissivity (after oxidation).

3.4.3 Total hemispherical emissivity (ε):

As for thermal conductivity, total hemispherical emissivity (ε) determinations have been carried out only on monoliths comprising $TaSi_2$ (total hemispherical emissivity values are deducted from spectral thermal emissivity measurements [22]). Emissivity values for oxidized materials at 1000°C are presented in figure 4 and the correlations for ε are given by the following expressions (in these formulas, T is in °C units):

- for $ZrB_2/SiC/TaSi_2$ (HP) $\varepsilon(T) = -2.9689\cdot10^{-10}\cdot T^3 + 2.4882\cdot10^{-7}\cdot T^2 + 2.3138\cdot10^{-4}\cdot T + 7.6225\cdot10^{-1}$ Eq. V
- for $HfB_2/SiC/TaSi_2$ (HP) $\varepsilon(T) = -7.5962\cdot10^{-10}\cdot T^3 + 1.0203\cdot10^{-6}\cdot T^2 - 2.2331\cdot10^{-4}\cdot T + 8.3449\cdot10^{-1}$ Eq. VI

In the temperature range studied, oxidized surfaces lead to emissivities higher than 0.8. This level of emissivity is entirely sufficient for the components for which UHTC monoliths are developed. In our applications, a high emissivity is indeed desirable, as it would reradiate much of the energy from the surface, eliminating some of the energy that the piece would otherwise have to handle.

3.5 Oxidation and thermal shock resistance

3.5.1 Furnace oxidation under stagnant air:

The thermal shock behaviour and the long time resistance (cumulative times up to 1000 hours) under oxidative atmosphere and high temperature have been assessed at 1000°C under stagnant air at atmospheric pressure by thermal treatments of several samples of all the materials sintered by HP in the first ATLLAS programme. For each material, more than 12 cycles of insertion/extraction (i.e. at least 24 thermal shocks) were achieved without any problems. In fact, the materials fully maintained their integrity. No cracks appeared and no destructive oxidation was observed. Thus, under the previous test parameters, all the compositions exhibited good thermal shock resistance. This is due to a large extent to the high thermal conductivity of these materials. Moreover, oxidation kinetics slow down with time and with the samples tested the total weight variations are very limited (< 0.3 % after 1000 h). In addition, as observed by SEM, there is formation of a protective layer on the surface. This protective layer is divided in two parts: a SiO_2 rich glass as the outermost coat (~7 µm thick) and an intermediate layer in the process of being oxidized (~20 µm thick). Thus, the selected materials exhibit good oxidation resistance with the test parameters and conditions of this study.

3.5.2 Arc-jet tests:

A test campaign was carried out under high-enthalpy hypersonic flow in an arc-jet facility at DLR Cologne (L2K) [23]. For each composition sintered by HP, four disc-shaped samples (Ø 26.5 mm, e = 4 mm) were machined in order to be able to check the materials' capabilities. Several tests were carried out from 1100 to 1500°C according to the following conditions:

sample A	*2 cycles*	*test of 300 s at 1100°C + test of 600 s at 1100°C*
sample B	*2 cycles*	*test of 300 s at 1100°C + test of 600 s at 1300°C*
sample C	*1 cycle*	*test of 600 s at 1400°C*
sample D	*1 cycle*	*test of 600 s at 1500°C*

The samples' resistance to high enthalpy flow was assessed by several measurements (weighing, thickness checking), and by photographs before and after each test and finally SEM observations of a few samples on both oxidized surfaces and polished cross-sections of discs (Figure 5). In addition, videos and photographs were recorded during all of the experiments (see for example Figure 6).

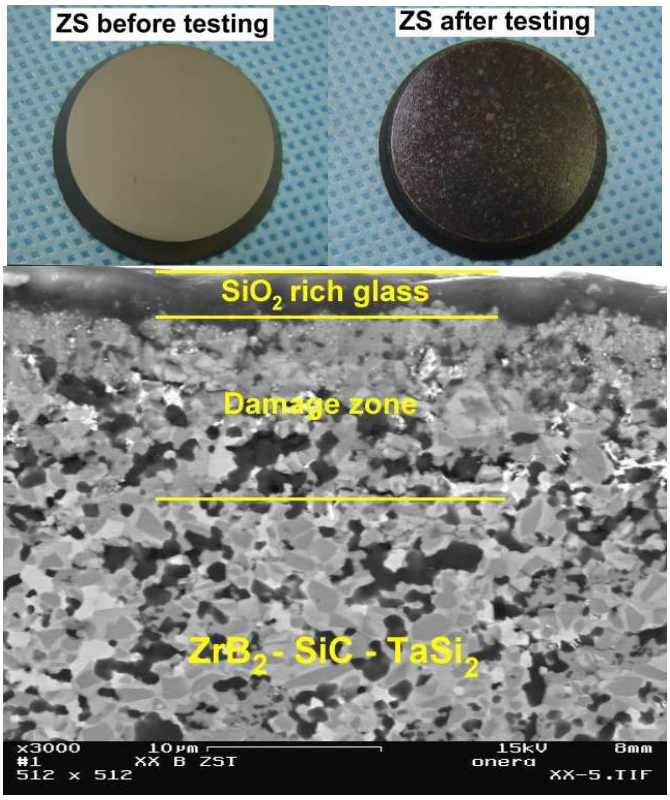

Figure 5 : ZrB_2/SiC disc before and after a test at 1500°C (top) and cross-sectioned. ZrB_2/SiC/$TaSi_2$ disc after 2 successive cycles at 1100 and 1300°C (bottom).

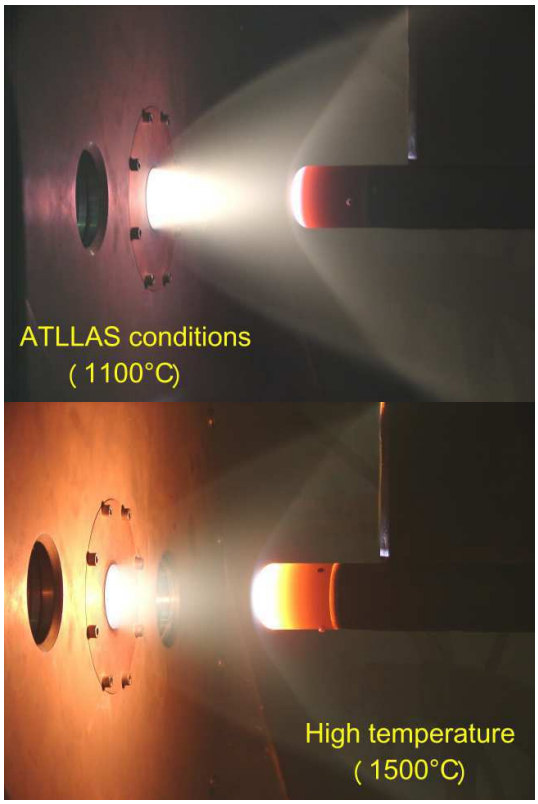

Figure 6 : Flow field around sample holder at different test conditions (shapes of the bow shock and the free stream boundary).

The results of this test campaign were very satisfactory. For each condition, good material resistance was detected (the most important mass and thickness variations observed during this campaign were quite limited: ΔM_{max} = 0.33% and Δe = 50 µm). As previously observed by SEM on oxidized materials (tests under stagnant air), there is again formation of a thin glass layer on the surface and underneath an intermediate layer in the process of being oxidized (SiC-depleted layer) [35]. Thermodynamically, ZrB_2, HfB_2 and SiC should oxidize when exposed to air. However, below 1200°C, it is reported in the literature that the oxidation of ZrB_2 (or HfB_2) is more rapid than that of SiC. Then there is production of a continuous protective oxide layer of B_2O_3 (l) with entrained ZrO_2 (or HfO_2) which prevents ZrB_2 (or HfB_2) from being further oxidized. At higher temperatures, B_2O_3 (l) evaporates due to its high vapour pressure and consequently the rate of SiC oxidation increases, inducing the formation of a SiO_2 rich glass on the surface [6]. Up to 1600°C, $TaSi_2$ addition improves oxidation resistance because it reduces oxygen vacancy concentration in ZrO_2.

In conclusion, cumulative durations up to 900 s are performed without any problems (for all the selected compositions). Very good sample-to-sample reproducibility and a lack of sensitivity to thermal load cycling have been demonstrated. In addition, all the selected materials are able to sustain high thermal loads (up to 1500°C/600 s). This good thermal-oxidative stability in severe environments is certainly one of the most important results of this work on UHTC materials.

4 CONCLUSION

Hypersonic and propulsion applications provide some unique thermal-structural challenges (sharp leading edges, air intakes, uncooled injectors, etc.). In order to fulfil the requirements of these components, some specific materials are compulsory: UHTCs. Indeed, thanks to their unique combination of mechanical, thermal and chemical properties, UHTCs are a promising technology for use in a number of high temperature structural applications.

In the ATLLAS and ATLLAS II projects, several compositions were and are always investigated. These materials are sintered by HP or FAST. They possess attractive properties: high hardness, high flexural stress, good machinability, high emissivity. Another attractive feature of these materials is their relatively high thermal conductivity which gives them better thermal shock resistance than most insulating materials and allows heat to be conducted from a hot point to a region of lower heating, where it could be re-radiated. In addition, these materials exhibit good resistance to oxidation at very high temperatures. All these properties allow these materials to fulfil the requirements to sustain hypersonic flight conditions as demonstrated in the ATLLAS project.

5 ACKNOWLEDGEMENTS

This work was carried out within two projects investigating high-speed transport: “Aerodynamic and Thermal Load Interactions with Lightweight Advanced Materials for High Speed Flight” and “Aero-Thermodynamic Loads on Lightweight Advanced Structures II”. These studies are coordinated by ESA-ESTEC and supported by the EU within the 6^{th} and 7^{th} Framework Programmes.

References

[1] M.M. OPEKA, I.G. TALMY and J.A. ZAYKOSKI - Oxidation-Based Materials Selection for 2000°C + Hypersonic Aerosurfaces: Theoretical Considerations and Historical Experience. Journal of Materials Science 39, 5887-5904, 2004.

[2] E. CLOUGHERTY, D. KALISH and E. PETERS - Research and Development of Refractory Oxidation Resistant Diborides. Technical Report AFML-TR-68-190, 1968.

[3] G. V. SAMSONOV - Refractory Transition Metal Compounds: High Temperature Cermets. Academic Press, New York, 1964.

[4] S.R. LEVINE, E.J. OPILA, M.C. HALBIG, J.D. KISER, M. SINGH and J.A. SALEM - Evaluation of Ultra-High Temperature Ceramics for Aeropropulsion Use. J. European Ceramic Society 22, 2757-2767, 2002.

[5] J. HAN, P. HU, X. ZHANG and S. MENG - Oxidation Behavior of Zirconium Diboride-Silicon Carbide at 1800 °C. Scripta Materialia 57, 825-828, 2007.

[6] W.G. FAHRENHOLTZ - Thermodynamic Analysis of ZrB_2-SiC Oxidation: Formation of a SiC-Depleted Region. J. American Ceramic Society 90, 43-148, 2007.

[7] F. MONTEVERDE and A. BELLOSI - Oxidation of ZrB_2-Based Ceramics in Dry Air. J. Electrochemical Society 150 [11], B552-B559, 2003.

[8] D.A. KONTINOS, K. GEE and D.K. PRABHU - Temperature Constraints at the Sharp Leading Edge of a Crew Transfer Vehicle. American Inst. of Aeronautics & Astronautics, 2001-2886, 2001.

[9] W.G. FAHRENHOLTZ, G.E. HILMAS, I. G. TALMY and J. A. ZAYKOSKI - Refractory Diborides of Zirconium and Hafnium. J. American Ceramic Society 90, 1347-1364, 2007.

[10] J. STEELANT – Atllas : Aero-Thermal Loaded Material Investigations for High-Speed Vehicles. 15th AIAA International Space Planes and Hypersonic Systems and Technologies Conference, Dayton, Ohio, 2008.

[11] http://www.esa.int/Our_Activities/Space_Engineering/ATLLAS_II_-_Project_summary

[12] J.F. JUSTIN - Investigations of High Temperature Ceramics for Sharp Leading Edges or Air Intakes of Hypersonic Vehicles. 3rd EUCASS, Versailles, France, CD-ROM ISBN 978-2-930389-47-8, 2009.

[13] J.F. JUSTIN and A. JANKOWIAK – Ultra High Temperature Ceramics: Densification, Properties and Thermal Stability. AerospaceLab, issue 3 – November 2011.

[14] A. EZIS and J.A. RUBIN - Hot Pressing. Engineered Materials Handbook, vol 4, Ceramics and Glasses, 186-193, 1991.

[15] G.E. GAZZA - Pressure Densification. Engineered Materials Handbook, vol 4, Ceramic and Glasses, 296-303, 1991.

[16] H.U. KESSEL and all - "Fast" Field Assisted Sintering Technology – A New Process for the Production of Metallic and Ceramic Sintering Materials.

[17] W.C. TRIP, H.H. DAVIS and H.C. GRAHAM - Effect of a SiC Addition of the Oxidation of ZrB_2. American Ceramic Society Bulletin, vol 52 [8], 612-616, 1973.

[18] E. OPILA and S. LEVINE - Oxidation of ZrB_2- And HfB_2-Based Ultra-High Temperature Ceramics: Effect of Ta Additions. Journal of Materials Science 39, 5969-5977, 2004.

[19] ASTM Standard E1876-09 - Standard Test Method for Dynamic Young's Modulus, Shear Modulus, and Poisson's Ratio by Impulse Excitation of Vibration.

[20] G.R. ANSTIS, P. CHANTIKUL, B.R. LAWN and D.B. MARSHALL - A Critical Evaluation of Indentation Techniques for Measuring Fracture Toughness: I. Direct Crack Measurements. J. American Ceramic Society 64, 534-553, 1981.

[21] W.J. PARKER, R.J. JENKINS, C.P. BUTLER and G.L. ABBOT - Flash Method of Determining Thermal Diffusivity, Heat Capacity, and Thermal Conductivity. J. Applied Physics 32, 1679-1684, 1961.

[22] D. DEMANGE and M. BEJET - New Methods for Measuring the Thermal Emissivity of Semi-Transparent and Opaque Materials. 8th International Conference on quantitative Infrared Thermography, Padova, 2006.

[23] B. ESSER - Thermal Characterisation of Onera's UHTC Materials. Deliverable D.3.2.6 of ATLLAS project, 2009.

[24] R. RIEDEL - Handbook of Ceramic Hard Materials. WILEY-VCH, 2000.

[25] N. FAULK - Electrical Discharge Machining. Engineered Materials Handbook, vol 4, Ceramics and Glasses, 371-376, 1991.

[26] S.Q. GUO and al - Mechanical Properties of Hot-Pressed ZrB_2-$MoSi_2$-SiC Composites. J. European Ceramic Society 28, 1891-1898, 2008.

[27] A.L. CHAMBERLAIN, W.G. FAHRENHOLTZ and G.E. HILMAS - High-Strength Zirconium Diboride-Based Ceramics. J. American Ceramic Society 87, 1170-1172, 2004.

[28] F. MONTEVERDE - Ultra-High Temperature HfB_2-SiC Ceramics Consolidated by Hot-Pressing and Spark Plasma Sintering. Journal of Alloys and Compounds 428, 197-205, 2007.

[29] F. MONTEVERDE, A. BELLOSI and L. SCATTEIA - Processing and Properties of Ultra-High Temperature Ceramics for Space Applications. Materials Science and Engineering: A. 485, 415-421, 2008.

[30] A. FRANCESE - Numerical and Experimental Study of UHTC Materials for Atmospheric Re-Entry. Dottorato di ricerca in ingegneria aerospaziale, 2007.

[31] R. LOEHMAN, E. CORRAL, H.P. DUMM and al - Ultra-High Temperature Ceramics for Hypersonic Vehicle Applications. Sandia Report, SAND 2006-2925, 2006.

[32] M. GASCH, S. JOHNSON and J. MARSCHALL - Thermal Conductivity Characterization of Hafnium Diboride-Based Ultra-High-Temperature Ceramics. J. American Ceramic Society 91, 1423-1432, 2008.

[33] Characteristics of Kyocera Technical Ceramics. http://americas.kyocera.com/kicc/pdf/Kyocera_Material_Characteristics.pdf.

[34] R. A. CUTLER - Engineering Properties of Borides. Engineered Materials Handbook, vol 4, Ceramics and Glasses, 787-803, 1991.

[35] T. PARTHASARATHY, R. RAPP, M. OPEKA and R. KERANS - A Model for the Oxidation of ZrB2, HfB2 and TiB2. Acta Materialia 55, 5999-6010, 2007.